Biosensors and Bioelectronics 268 (2025) 116880

Contents lists available at ScienceDirect

Biosensors and Bioelectronics

journal homepage: www.elsevier.com/locate/bios

α-Synuclein plastic antibody applied to monitor monomeric structures and discriminate aggregated forms in human CSF

Inês S. da Silva [a], Ana R. Cardoso [a], Lasse Reimer [b,c], Annekatrin König [d], Christoph van Riesen [e], Tiago Fleming Outeiro [d,f,g,h], Poul Henning Jensen [b,c], M. Goreti F. Sales [a,*]

[a] BioMark@UC/CEMMPRE-ARISE, Department of Chemical Engineering, Faculty of Sciences and Technology, University of Coimbra, Coimbra, Portugal
[b] Danish Research Institute of Translational Neuroscience – DANDRITE, Aarhus University, Aarhus, Denmark
[c] Department of Biomedicine, Aarhus University, Aarhus, Denmark
[d] Department of Experimental Neurodegeneration, Center for Biostructural Imaging of Neurodegeneration, University Medical Center Göttingen, Waldweg 33, 37073, Göttingen, Germany
[e] Department of Neurology, University Medical Center Göttingen, Göttingen, Germany
[f] Max Planck Institute for Multidisciplinary Sciences, Göttingen, Germany
[g] Translational and Clinical Research Institute, Faculty of Medical Sciences, Newcastle University, UK
[h] Scientific Employee with an Honorary Contract at German Center for Neurodegenerative Diseases (DZNE), 37075, Göttingen, Germany

ARTICLE INFO

Keywords:
Alpha-synuclein
Plastic antibody
Electrochemical biosensor
Carbon screen-printed electrodes
Parkinson's disease

ABSTRACT

Aggregation of alpha-synuclein (aSyn) occurs in presynaptic neurons and constitutes a key factor for the progression of Parkinson's disease, emphasising the urgency of early detection to support effective treatment. Unfortunately, a reliable, sensitive and cost-effective diagnostic tool has so far been lacking.

Thus, this work presents a novel biosensor for detecting aSyn using plastic antibodies coupled to electrochemical detection. This biosensor was designed for portability and compatibility with point-of-care devices and exploits the electropolymerization of methylene blue (MB) together with aSyn on the carbon working electrode of screen-printed electrodes (SPEs). By electrochemical impedance spectroscopy (EIS) measurements, the sensor showed exceptional analytical performance in detecting aSyn monomers in human CSF samples. It showed a linear trend of response from 1 fM to 10 pM with an impressively low limit of detection of 69 aM. Selectivity tests confirmed the predominant response to aSyn monomers, a less intense response to oligomers and insensitivity to fibrils.

Overall, this plastic antibody-based electrochemical sensor represents a significant breakthrough as it is the first of its kind to accurately, sensitively and selectively detect aSyn monomers with a partial response to oligomers. Its simplicity and reproducibility promise to contribute to the early and effective diagnosis of Parkinson's disease.

1. Introduction

Parkinson's disease (PD) is a chronic and progressive neurodegenerative disease, of increasing prevalence. (Zhu et al., 2024; Van Den Eeden et al., 2003). It is linked to a loss of dopaminergic neurons in the *substantia nigra pars compacta*, leading to motor symptoms (as resting tremor, rigidity and bradykinesia) and non-motor symptoms (constipation, behavioural disturbances during REM sleep and hyposmia) (Postuma and Berg, 2017; Fearnley and Lees, 1991). Neuropathologically, PD has intraneuronal inclusions that are known as Lewy bodies and Lewy neurites, consisting mainly of α-synuclein (aSyn) (Spillantini M. G., Schmidt M. L., Lee V. M., Trojanowski J. Q. and M., 1997). aSyn is a small, soluble, intrinsically disordered protein of 140 amino acid residues (14 kDa) encoded by the *SNCA gene* (Eliezer et al., 2001; Maroteaux et al., 1988; Xia et al., 1996). Mutations in the *SNCA* gene and gene duplications/triplications cause familial forms of PD and increase the risk of developing the disease (Koukouraki and Doxakis, 2016; Polymeropoulos et al., 1997). Currently, the diagnosis of PD is achieved based on the assessment of clinical symptoms, which may be unclear in the early stages, leading to possible misdiagnosis (Donadio et al., 2014; Hughes et al., 1992).

aSyn is emerging as a candidate biomarker for PD. The protein is

* Corresponding author.
E-mail addresses: goreti.sales@eq.uc.pt, goreti.sales@gmail.com (M.G.F. Sales).

https://doi.org/10.1016/j.bios.2024.116880
Received 26 July 2024; Received in revised form 20 October 2024; Accepted 24 October 2024
Available online 6 November 2024

detectable in various readily available body fluids, including cerebrospinal fluid (CSF), plasma or serum, and tear fluid (Anderson et al., 2006; El-agnaf et al., 2006; Maass et al., 2020). While there has been interest in assessing seed-competent, aggregated forms of aSyn (Siderowf et al., 2023), the detection of the total levels of aSyn in PD is also important for several reasons. As a biomarker, it was recently shown that the levels of aSyn in PD and in individuals at risk are increased in brain-derived extracellular vesicles in blood (Yan et al., 2024). Moreover, exposure of the N-terminus of monomeric aSyn influences its aggregation propensity (Stephens et al., 2020), and it is likely that increased levels of aSyn will fuel aggregation into oligomeric and fibrillar species. In this context, measuring monomeric/total aSyn is valuable for inferring on possible pathological alterations. Thus, it is important to devise sensitive and accessible assays to measure the levels of monomeric/total aSyn, to complement information obtained by measuring aggregated forms of the protein.

Biosensors are widely used for biomarker detection due to their advantages such as speed, sensitivity and cost-effectiveness compared to traditional techniques such as enzyme-linked immunosorbent assay (ELISA) or Western blot (An et al., 2010; Liu et al., 2017). Electrochemical immunosensors for the detection of aSyn have been reported in which an FTO-based electrode was modified with cysteamine and anti-aSyn (Md. ChuangYe Ge, Mahbubur Rahman, Wei Zhang, Nasrin Siraj Lopa and Sujin Yoon, Hohyoun Jang, Xu Guang-Ri, 2020; Xu et al., 2015). These devices displayed a linear trend of response from 10 to 1000 ng/mL, but the antibodies used did not discriminate between monomeric and aggregated forms. Using molecularly imprinted polymer technology, synthetic antibodies can be produced as an alternative to natural antibodies. These synthetic counterparts are inexpensive, stable and highly sensitive (Ana R. Cardoso et al., 2019a,b).

According to the recent literature, there are some studies on electrochemical biosensors for aSyn (Hassan et al., 2019; Silva et al., 2024), from which only few are based on plastic antibodies (Pilvenyte et al., 2023). These are detailed in Table 1. Existing studies use conventional electrodes made of carbon (Ma et al., 2020), gold (M. Lee et al., 2021; M. H. Lee et al., 2021) or ITO (Lee et al., 2020). Some approaches use highly conductive materials based on conjugated microporous polymers and graphene nanosheets to alter glassy carbon electrodes (GCEs) for detecting aSyn in human serum (Ma et al., 2020). The plastic antibody material was prepared by electropolymerization of pyrrole and showed selectivity for aSyn when tested against its beta and gamma isoforms, although no aggregation information was provided. In another approach, different ratios of 3,4-ethylenedioxythiophene (EDOT) and hydroxymethyl-EDOT (EDOT-OH) were copolymerized on an ITO surface to detect the aSyn peptide in the culture medium of differentiating midbrain-like organoids (Lee et al., 2020). This sensor was tested for possible interference by human serum albumin (HSA), but further testing is required to confirm its selectivity in CSF samples. In two other studies, aSyn peptide sequences were used as templates to detect the protein in human brain organoids by electropolymerization of aniline/*m*-aminobenzenesulfonic acid (AN/MSAN) on Au electrodes under specific conditions (M. Lee et al., 2021; M. H. Lee et al., 2021). In one study, transition metal dichalcogenides (TMDs) were used to increase the conductivity and HSA was combined with aSyn to test for possible interference.

None of the current electrochemical-based biosensors targeting aSyn assess the sensor's response to the protein's level of aggregation, a critical factor for accurate screening. This information is crucial for physicians as the diagnosis and prognosis of PD depends on knowing the extension of aSyn aggregation. Furthermore, to effectively screen for monomeric forms of aSyn, it is essential to use monomeric aSyn in the imprinting phase to avoid detecting aggregated forms. Given the increasing prevalence of PD, biosensors should be designed as portable devices to enable point-of-care (PoC) diagnostics. Thus, in the present study, a novel electrochemical biosensor containing a new plastic antibody targeting monomeric forms of aSyn is presented. This biosensor utilizes a multifunctional compound capable of forming multiple interactions with the target peptide, resulting in an imprinted polymer film.

Thus, this study details the modification of carbon SPEs through the bulk electropolymerization of methylene blue (MB) around monomeric aSyn. MB contains aromatic rings that can undergo electropolymerization and amine functional groups that enable electrostatic interactions with the protein, thereby contributing to the formation of the imprinted cavity within a polymeric matrix. As far as we know, we reported the first use of MB as monomer for protein imprinting in Synuclein (2022) Meeting (Proceedings of Synuclein Meeting 2022), which were the first steps of this whole manuscript, with two other papers using it for detecting small molecules (melatonin and chlorpromazine) (Liu et al., 2022; Sunon and Ngamchuea, 2023). The sensor surface modification was characterized using cyclic voltammetry (CV), electrochemical impedance spectroscopy (EIS), and square-wave voltammetry (SWV). Calibration curves of various aSyn-imprinted and non-imprinted polymer-coated electrodes were recorded. Finally, the sensor's application was tested on spiked human cerebrospinal fluid (CSF) samples.

2. Materials and methods

2.1. Synthesis of monomers, oligomers, and fibrils of alpha-synuclein

2.1.1. Production and purification of peptides

Human recombinant aSyn was extracted and purified from transformed BL21(DE3)-competent cells according to previously established

Table 1
Comparison of developed molecularly imprinted polymers for detecting α-synuclein.

Monomer	Target imprint	Electrode material	Assembly	Potential range	Linear range	LoD	Reference
AN and MSAN	Peptide sequence from aSyn	Gold	AN and MSAN, electropolymerized to poly(AN-co-MSAN) on Au electrodes	–	69.4 aM - 69.44 fM	0.694 fM	(M. Lee et al., 2021)
AN and MSAN	Peptide sequence from aSyn	Gold	AN and MSAN with TMDs, electropolymerized to poly(AN-co-MSAN) on Au electrodes	−0.6 to 0.6 V at a scan rate of 100 mV s^{-1}	0.07 fM - 7.1 pM	0.04 fM	(M. H. Lee et al., 2021)
EDOT and EDOT-OH	Peptide sequence from aSyn	ITO glass	EDOT and EDOT-OH copolymerized as poly (EDOT-*co*-EDOT-OH).	−0.6 V–1.1 V at a scan rate of 100 mV s^{-1}	0.065 pM - 0.65 nM	4 pM	Lee et al. (2020)
Pyrrole	aSyn	GCE	GCE/GS/CMP/GA/aSyn. Electropolymerization of pyrrole. NaOH solution	−0.35 V–0,85 V at a scan rate of 50 mV s^{-1}	6.94 fM - 555.6 pM	2.43 fM	Ma et al. (2020)
MB	aSyn	Carbon SPE	Carbon SPE/MB and aSyn monomers/oxalic acid	−0.3–0.7 V at a scan rate of 50 mV s^{-1}	1 fM −10 pM	68.8 aM	This work

AN: aniline; CMP: conjugated microporous polymer; EDOT: 3,4-Ethylenedioxythiophene; EDOT-OH: hydroxymethyl EDOT; GA: glutaraldehyde; GCE: glassy carbon electrode; GS: graphene nanosheets; ITO: Indium tin oxide; LoD: limit of detection; MB: methylene blue; MSAN: *m*-aminobenzenesulfonic acid; NaOH: sodium hydroxide; aSyn: alpha-synuclein; SPE: screen-printed electrode; TMDs: transition metal dichalcogenides.

methods (Reimer et al., 2022). Oligomers were prepared according to the method described in (Kumar et al., 2020). Fibrils were prepared using llyophilized recombinant aSyn monomer, which was resuspended in sterile PBS (Gibco) to a final concentration of 5 mg/mL and maintained in an Eppendorf Thermotop shaker at 37 °C, 1050 rpm for 5 days to induce fibrillization as previously described in (Ruesink et al., 2019).

2.2. Methods for alpha-synuclein characterization

2.2.1. Antibodies

α-Syn mouse monoclonal antibody was purchased from Biosciences; the α-Syn aggregate-specific rabbit monoclonal antibody (MJF14) was purchased from Abcam; the fibril-specific antibody FILA5 (rabbit polyclonal antibody) was referenced in (Lindersson et al., 2004). Two secondary antibodies were used: horseradish peroxidase (HRP)-conjugated rabbit polyclonal anti-mouse antibody (Dako, P0260) and HRP-conjugated porcine polyclonal anti-rabbit antibody (Dako, P0217)

2.2.2. Thioflavin T assays

0.5 μg aSyn monomer, oligomer, preformed fibrils and the biophysical nature of aSyn, PBS or were assayed for thioflavin T (ThT) signaling as previously described in (Ruesink et al., 2019).

2.2.3. Dot blot test

Dot blots were performed as previously described according to (Ruesink et al., 2019). The quantification of the blot was performed using ImageJ.

2.3. CSF samples

The CSF was obtained from a male control patient who showed no signs of neurodegenerative, neuroinflammatory or neurooncological diseases.

2.3.1. Ethical statement

The local ethics committee approved before the study began. Both patients gave their written consent. CSF samples were collected according to published protocols (Teunissen et al., 2009).

2.4. Biosensor assembly, analysis and evaluation

2.4.1. Apparatus

The electrochemical tests were carried out using a PalmSens4 potentiostat/galvanostat operated with PSTrace 5.8 software. The SPEs used in the experiments were commercial products from Metrohm DropSens, specifically DRP-110. These SPEs had 3-electrode systems, as a carbon counter (CE) and working electrode (WE) and a silver reference electrode (RE). The electrodes were connected to the potentiostat via a PalmSens switch box.

2.4.2. Reagents and solutions

All chemicals compounds used were of analytical grade and the solutions were prepared with high purity Milli-Q water (conductivity <0.1 μS/cm) of laboratory quality. The chemical reagents were used according to (A. R. Cardoso et al., 2019a,b), sulfuric acid 95–97% from Honeywell Fluka, methylene blue (MB) from Merck, oxalic acid 98% from Acros Organic, glucose from Alfa Aesar and urea from Fisher bioreagents.

A fresh 1 mM solution of MB was prepared in 10 mM phosphate buffered saline (PBS) at pH 7.4. In addition, solutions of 500 mM sulfuric acid and 500 mM oxalic acid were prepared with highly purified Milli-Q water. Electrochemical tests were performed with 5.0 mM ($K_3[Fe(CN)_6]$)/($K_4[Fe(CN)_6]$) at pH 7.4 in 10 mM PBS. Each aSyn standard solution was prepared in 10 mM PBS (pH 7.4); aSyn solutions contain the monomeric form, unless stated otherwise. The human cerebrospinal fluid (CSF) samples were also diluted in 10 mM PBS (pH 7.4).

2.4.3. Electrochemical measurements and procedures

All electrochemical tests were carried out in triplicate. The electrochemical measurements used in this work were according to (Serrano et al., 2022).The data analysis were made by (Serrano et al., 2022).

Electrode surface modification was made by three electrochemical measurements mentioned in (Serrano et al., 2022). using a redox probe solution of 5.0 mM ($[Fe(CN)_6]^{3-}$)/($[Fe(CN)_6]^{4-}$) in 10 mM PBS buffer at pH 7.4. Curve fitting was generated using EIS assays with standard solutions of aSyn protein in PBS and CSF samples (diluted 1:1000 in PBS buffer) ranging from 0.1 fM to 1 nM. The analytical performance of the sensor against different forms of aSyn (monomers, oligomers and fibrils) at a concentration of 0.1 pM was assessed in the selectivity evaluation. The protein concentration was measured using the bicinchoninic acid (BCA) assay (Pierce), with a 30-min incubation period (Reimer et al., 2022). The limit of detection (LoD) was determined by finding the point where the two linear segments of the electrical response versus concentration curve intersect. (Harvey, 2000).

2.4.4. Biosensor assembly

The electrochemical biosensor was constructed using the molecular imprinting technique, as shown in Fig. 1. The assembly was carried out on commercially available carbon SPEs and all tests were performed in triplicate. The setup started with cleaning the electrodes by CV (−0.2 to +1.0 V; at a scan rate of 100 mV/s; 30 cycles) in a 500 mM sulfuric acid solution. The electrodes were then rinsed and dried in a nitrogen atmosphere. The resulting electrochemical response was measured using a standard solution of 5.0 mM ($K_3[Fe(CN)_6$/($K_4[Fe(CN)_6]$) in PBS buffer. The plastic antibody was formed by electropolymerization in a solution containing 1 mM MB and 0.1 μM synthetic aSyn protein using chronoamperometry (150 s at −0.15 V) at room temperature (~25 °C). Prior to this step, the MB solution was deoxygenated with nitrogen gas for 1 min. For the control polymer, the same procedure was performed without the protein. After the polymerization step, the electrode was treated with PBS by CV (−0.4 to +1.0 V; scan rate of 100 mV/s; 10 cycles) to stabilize the surface. The sensor layer was then washed and dried in a nitrogen atmosphere.

The electrochemical changes on the sensor surface were analysed using the standard redox probe solution ($K_3[Fe(CN)_6]$/$K_4[Fe(CN)_6]$) in buffer solution. The WE was then incubated with 6 μL of a 500 mM oxalic acid solution for 1 h to remove the protein and create voids. After another round of washing and drying, the response of the sensor was again compared to the standard redox probe solution. Finally, PBS buffer solution was drop casted on the electrode and CV scanning was used (−0.4 to +0.3 V; scan rate of 100 mV/s; 20 cycles) to stabilize the sensor surface. The tested SPEs were then stored overnight in a refrigerator at 4 °C.

2.4.5. Performance of the analytical of the plastic antibody

The evaluation of analytical performance of the sensing layer in PBS buffered solutions was made as in (A. R. Cardoso et al., 2019a,b). The protein concentrations varied from 0.1 fM to 1 nM, all within the same linear range and tests were performed in triplicate. For CSF samples, standard solutions used human CSF control samples diluted 1:1000 in PBS buffer as background, in the same concentration range of aSyn. The time of incubation was set to 30 min.

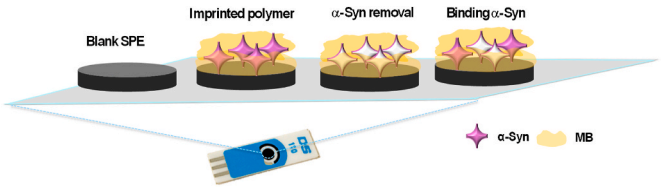

Fig. 1. Schematic representation of assembly of the plastic antibody by molecular imprinting technology on the carbon SPE.

3. Results and discussion

3.1. Protein characterization

The biophysical properties of the α-synuclein (aSyn) species used in this study were evaluated using thioflavin T-binding assays for the monomeric, oligomeric and fibrillar forms of aSyn. aSyn oligomers exhibited a higher β-sheet content than monomeric aSyn, although significantly less than that of preformed aSyn fibrils (Fig. 2A). Dot-blot analysis with antibodies that bind to the entire aSyn (Syn-1) and to the aggregated aSyn conformations (FILA-5 and MJFR-14-6-4-2) showed that aSyn monomers were recognised exclusively by the Syn-1 antibody. In contrast, aSyn oligomers and preformed fibrils were recognised by all three antibodies (Fig. 2B). In particular, the preformed fibrils were better recognised by MJFR-14-6-4-2 and especially by FILA-5 than the oli gomers (Fig. 2C and D). These results and the thioflavin T binding data suggest that the oligomers used in this study are an intermediate species between monomeric and fibrillar aSyn and structurally resemble monomers rather than fibrils. This distinction was used to identify the different forms of aSyn (monomeric, oligomeric and fibrillar aSyn) in contact with the sensory layer. This emphasises the importance of distinguishing between these forms — an ability that current biosensors lack.

3.2. Biosensor assembly

The WE was modified according to the schematic diagram in Fig. 1 and monitored by CV, EIS and SWV assays using a standard redox probe. Initially, the carbon SPEs were treated with a sulfuric acid solution to eliminate surface contaminants and oxidize the carbon surface (making it more hydrophilic) (Rebelo et al., 2016a, 2016b). Overall, the resulting electrochemical data signalled increasing current peaks and decreasing Rct values after cleaning (Fig. S1). The oxidation peaks as obtained by CV had average current values of 124.67 ± 3.86 μA; the average R_{ct} values in EIS were 309.93 ± 6.48 Ω; and the average current in SWV was 70.09 ± 5.55 μA.

After the cleaning process, the electrode surface underwent bulk polymerization through the addition of methylene blue (MB) and the monomeric form of aSyn. "Specifically, the oxidation peaks of MB and aSyn were −0.25 V and +0.63 V, respectively (Fig. S2). The use of a potential range encompassing both potentials would generate radicals of both species and induce their copolymerisation, irreversibly trapping aSyn in a polymer matrix (Liu and Mu, 1999). Therefore, the use of cyclic voltammetry (normally used in the polymerization of MB) (Brett et al., 1999) could lead to partial oxidation of aSyn as a large potential range is involved. Instead, chronoamperometry was used to prevent chemical modification of aSyn. It allowed the use of a single potential value that led to the oxidation of (only) MB, ensuring the formation of radical MB species and thus stimulating the electropolymerization of aSyn." Moreover, poly(MB) is a semiconductive polymer that facilitated electron transfer on the electrode surface, resulting in reduced charge-transfer resistance and enhanced sensitivity (Karyakin et al., 1993). Electrochemical assays confirmed the formation of poly(MB) polymer (Fig. S1). CV data demonstrated increasing current values (145.33 ± 2.87 μA); EIS data showed a marked reduction in R_{ct} values (18.3 ± 1.88 Ω); and SWV data revealed a significant increase in current (126 ± 2.83 μA) compared to the initial values.

Following polymerization, the template aSyn was removed to generate imprinted cavities capable of binding aSyn in samples. This was achieved through by acidic treatment with oxalic acid on the WE, followed by electrochemical readings (Fig. S1). CV data (Fig. S1D) exhibited minimal variation compared to electropolymerization readings (141.33 ± 1.70 μA), being the least sensitive technique used; EIS data (Fig. S1E) demonstrated an increase in Rct values to 47.12 ± 6.84 Ω, opposite to the response during polymer formation; and SWV (Fig. S1F) indicated a decrease in current to 114.33 ± 4.50 μA.

In parallel to the plastic antibody assembly, a control non-imprinted material was assembled. As shown in Fig. S1, the electrochemical

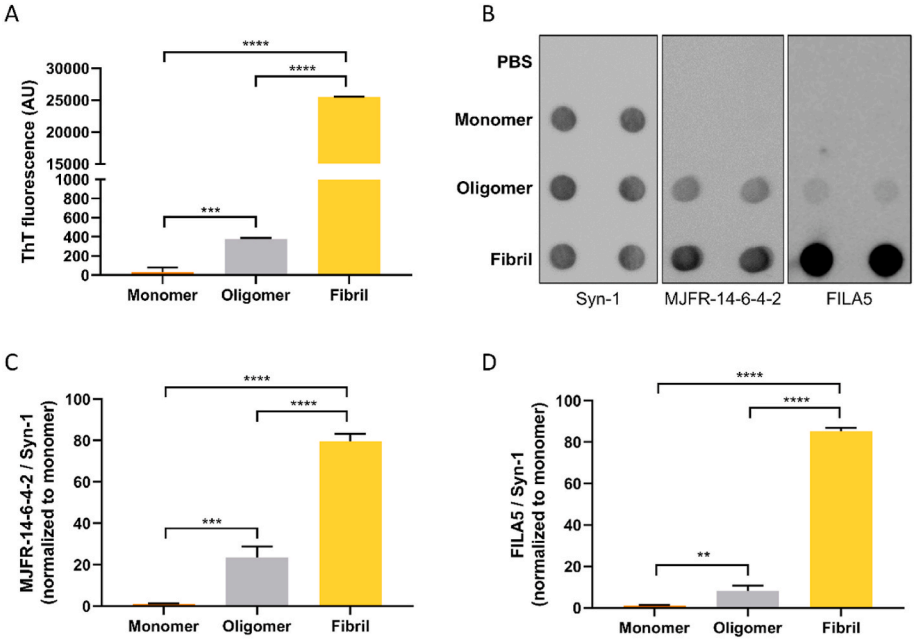

Fig. 2. A) Thioflavin T fluorescence signal of PBS or 0.5 μg α-syn monomer, oligomer or preformed fibril (excitation at 450 nm and emission at 486 nm). The background PBS measurement was subtracted from the signals of α-syn monomer, oligomer and preformed fibril. Thioflavin T fluorescence signal is represented in arbitrary units (AU). Figure shows mean ± SD of three independent experiments (***$p < 0.001$, ****$p < 0.0001$, one-way ANOVA followed by Tukey's multiple comparisons test). B) Representative image of antigenicity of PBS, α-syn monomers, oligomers, and preformed fibrils to Syn-1 (total α-syn antibody), MJFR-14-6-4-2 (aggregation-specific α-syn antibody) and FILA5 (fibril α-syn specific antibody) was determined using dot blot. Dots consists of 100 ng protein spotted in duplicates. C and D) Quantification of MJFR-14–6-4–2/Syn-1 (C) or FILA5/Syn-1 (D) α-syn signal ratio normalized to monomer signal. Figures show mean ± SD of three independent experiments (**$p < 0.01$, ***$p < 0.001$, ****$p < 0.0001$, one-way ANOVA followed by Tukey's multiple comparisons test).

responses indicated similar chemical modifications in the non-imprinted material, though the changes observed in CV, EIS, and SWV were slightly more pronounced compared to the imprinted version. These results were attributed to more extensive polymer formation in the absence of the protein. By not having aSyn within the monomers in solution, the polymer chains are under more favourable conditions for growth, as aSyn does not hinder the addition of monomers to the growing chains. After completion of the removal step, the electrochemical data displayed slight differences from the controls, indicating the removal of unreacted reagents or loosely bound oligomeric structures during the acidic wash.

Overall, the poly(MB) functioned as a conductive polymer under the tested conditions, resulting in increased current and decreased resistance values. The imprinted and control materials demonstrated differences related to the presence of the target protein, with more extensive polymer formation observed in the control material. The removal of aSyn from the imprinted polymer partially reversed the polymerization effects, as expected.

3.3. Analytical performance in PBS

Evaluation of the analytical performance of the sensor by incubation of the WE with increasing concentrations of monomeric aSyn standard solutions. Following each incubation, the 3-electrode system was washed, and the electrochemical measurements taken by casting the iron redox probe prepared in PBS. The results are calibration data plotted Rct against the logarithm of the protein concentration.

The EIS measurements of the plastic antibody showed that higher protein concentrations led to an increase in the diameter of the semicircles in the Nyquist plots, which indicates an increase in the electrical surface resistance (Fig. 3-C). The biosensor showed a linear trend of 1.0 fM and 0.10 nM, with an average slope of 25.31 Ω/decade and a standard deviation of ~0.86%. At higher protein concentration, the sensing layer reached saturation. The reproducibility of the sensor was evaluated by performing at least three independent tests with different SPE units, achieving a squared correlation coefficient of at least 0.99 for all calibrations (Fig. 3-D). The electrochemical response demonstrated excellent reproducibility, with relative standard deviation (RSD) values ranging from~0.72% to ~4.09%. Overall, these findings confirmed that this plastic antibody is highly sensitive for detecting the monomeric aSyn, with an impressive LoD of 0.18 fM.

Parallel measurements were performed using non-imprinted control devices to assess the non-specific response of the sensing layer (Fig. 3-A). Generally, the control sensor responses were random in relation to the increasing protein concentration across all tested SPEs (Fig. 3-B). Consequently, these results indicated that the control electrodes were unable of detecting aSyn monomers, in any of the tested concentrations, thereby demonstrating negligible non-specific interactions between the protein and the surface of the carbon electrode.

3.4. Sensor analytical performance in CSF samples

Given that CSF is a highly promising biofluid for the detection pf aSyn and the diagnosis of synucleinopathies, the analytical performance of the sensor layer was evaluated with CSF control samples. This approach also provides valuable insights into the behavior of the electrodes when operating with real samples. For these assays, the CSF samples were diluted 1:1000 in 10 mM PBS (pH 7.4). Each assay was performed in triplicate. Analytical characteristics were derived by plotting calibration curves of charge transfer resistance (Rct) from EIS measurements against the logarithm of the protein concentration (Fig. 4-B,D). The imprinted sensor displayed linear response over the

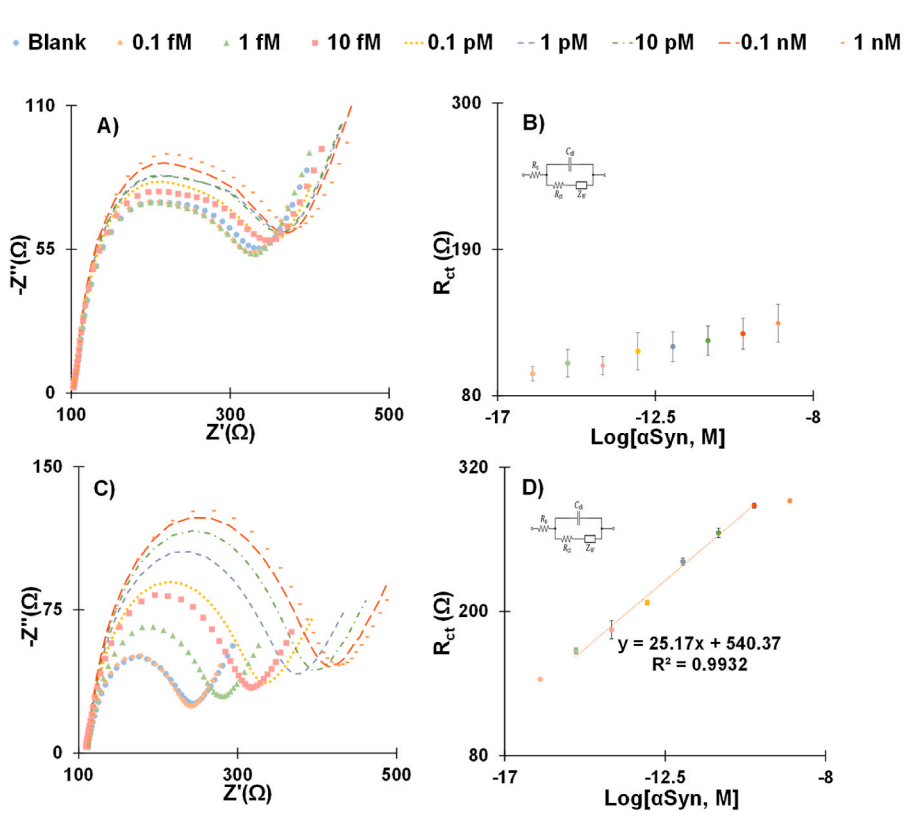

Fig. 3. Nyquist plots (A,C) of the EIS measurements and the corresponding calibration curves (B,D) of SPEs containing the plastic antibody (C,D) and the control material (A,B), in 5.0 mM ($K_3[Fe(CN)_6]$/($K_4[Fe(CN)_6]$) in 10 mM PBS buffer (pH 7.4). Standard solutions were prepared in PBS buffer with different concentrations of monomeric aSyn. Data represent the mean ± SD of three independent devices.

range of 1.0 fM to 10 pM, with the standard deviation of the calibration slope being ~0.53%, for a slope average of 41.69 Ω/decade concentration; the squared correlation coefficient for all calibrations was 0.99 (Fig. 4-D). The reproducibility of the system was confirmed by relative standard deviation (RSD) values ranging from ~3.22% to ~5.6%, showing a linear trend. Compared to results obtained in buffer, the use of CSF blank solutions produced more sensitive responses for monomeric aSyn, with an excellent limit of detection (LoD) of 68.8 aM. Therefore, this sensor is applicable in the real PD detection scenarios. In PD patients the reference concentration of aSyn in CSF samples is at the ng/mL level, which is significantly higher than the concentrations in healthy control subjects, which are in the range of pg/ml (Eusebi et al., 2017; Kapaki et al., 2013; Shalash et al., 2017).

In parallel, equivalent measurements were conducted using control sensors to evaluate the imprinting process and monitor the non-specific response of the sensor layer (Fig. 4-A). Similar to the calibrations with PBS, the response of the controls exhibited random responses against to increasing protein concentrations across all tested devices (Fig. 4-B). These results indicate that the control sensor was unable to detect aSyn monomers, in any of tested concentrations, demonstrating that this sensor exhibited negligible non-specific interactions between the protein and the carbon surface.

3.5. Selectivity for the monomeric form of α-syn

Selectivity studies were performed to determine the selectivity of the sensor for the monomeric form of aSyn were conducted by testing the plastic antibody-based sensor independently against monomers, oligomers, and fibrils. For this purpose, the different protein forms were incubated on the WE at a concentration of 0.1 pM for 30 min. Data analysis involved plotting the Rct values from EIS measurements against the logarithmic concentration of the various aSyn forms (Fig. 5). The results indicated that the imprinted sensor was unable to detect fibrils (with a blank relative difference of 4.46 ± 1.93%), likely due to the more complex, condensed, and larger structure of fibrils, which do not fit into the polymer-formed cavities (Kumari et al., 2021). While the sensor could recognize oligomers (with a blank relative difference of 35.16 ± 1.41%), this response was not as significant compared to that for monomers (with a blank relative difference of 49.27 ± 2.46%). This

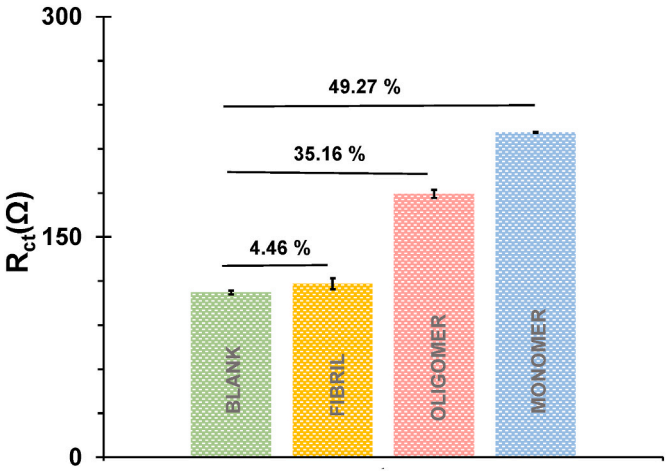

Fig. 5. Absolute Rct values of three different imprinted-based sensors obtained for 0.1 pM aSyn standard solutions in different forms (monomers, oligomers, and fibrils). Error bars represent the mean ± SD of at least 3 independent devices.

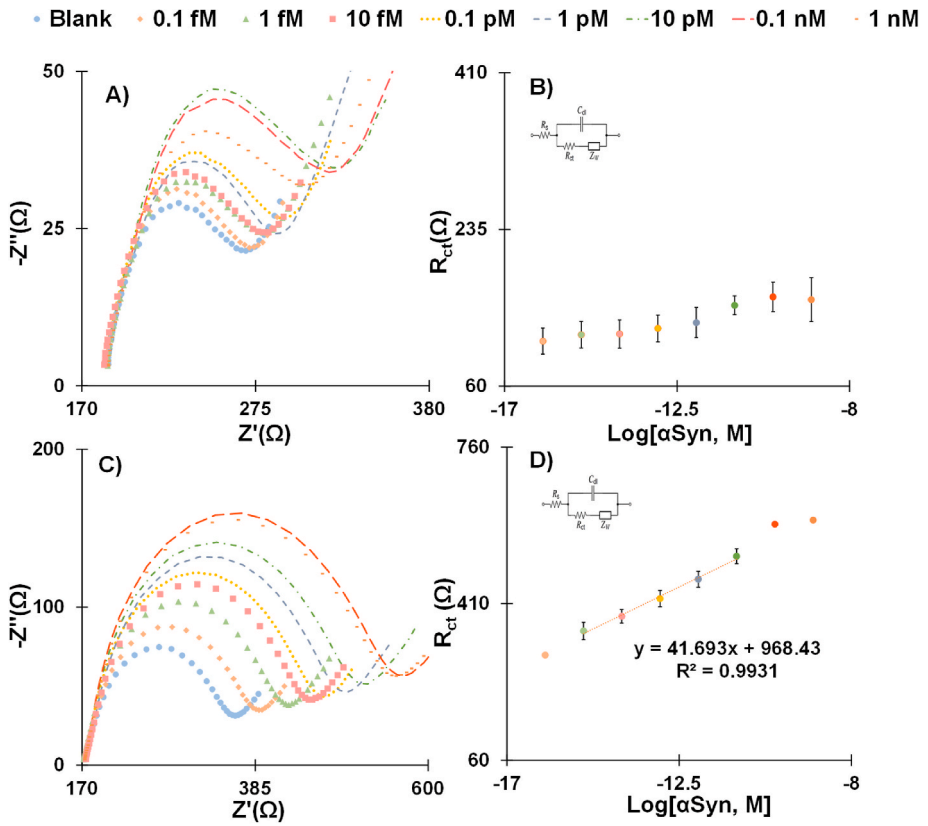

Fig. 4. Nyquist plots (A,C) of the EIS measurements and the corresponding calibration curves (B,D) of SPEs containing the plastic antibody (C,D) and the control material (A,B), in 5.0 mM $(K_3[Fe(CN)_6])/(K_4[Fe(CN)_6])$ in 10 mM PBS buffer (pH 7.4). Standard solutions were prepared in a background of CSF diluted 1:1000 in PBS buffer with different concentrations of monomeric aSyn. Data represent the mean ± SD of three independent devices.

can be attributed to oligomers being an intermediate form in the protein aggregation process, where small oligomers have a structure not drastically different from monomers (Li et al., 2019). Selectivity tests with other components in the CSF besides oligomers/fibrils were not performed, as the previous calibrations in diluted CSF showed negligible interference of the combination of all components.

Overall, the developed electrochemical sensor based on plastic antibodies showed a high selectivity for aSyn monomers and was able to effectively monitor them in CSF samples in which the presence of fibrils is excluded in principle. The sensor detects more intensively to monomeric forms than to oligomers, so the levels detected can be attributed to both forms in the case of unknown samples. This further emphasises the need to evaluate the different forms of aggregation in the detection of aSyn and also questions the validity of previous work where studies were performed with aSyn in uncontrolled levels of aggregation.

In general terms, the selectivity of the imprinted sensor was also evaluated by testing the response of the plastic antibody on the carbon SPE to other components in CSF. Glucose and urea were used for this experiment as they dominate this biological fluid. These compounds were tested in mixed solutions of aSyn and interfering compound and compared with a solution containing only aSyn (1.0 pM). Each solution was incubated on the WE for 30 min. The results shown in Fig. S3B indicate little interference from glucose ($-2.8 \pm 7.3\%$) and urea ($-12.6 \pm 4.0\%$), thereby confirming the good selectivity of the plastic antibody for aSyn.

Moreover, to assess the usefulness of the sensor, spiked CSF samples were tested, checking the behaviour of the system at different concentration levels of aSyn. Specifically, concentrations of 0.1, 1.0 and 10 pM spiked aSyn over blank CSF samples were analysed by extrapolation at the calibration curve, and the observed errors were of +7.3, −5.6 and −4.8%. Further testing would be required in CSF samples from PD patients to which the authors did not have access at the time of publication.

4. Conclusions

This work presents for the first time a sensor based on plastic antibodies that can detect the monomeric form of the protein aSyn with high sensitivity, selectivity and reproducibility. Previous works reported do not mention which form of a-Syn is being employed, although this is critical in clinical terms. The electrochemical sensor is assembled with a plastic antibody on standard carbon SPEs, involving the bulk polymerization of MB in the presence of the target protein. The resulting sensor showed exceptional sensitivity for aSyn monomers, covering a linear range from 1 fM to 10 pM and achieving an impressive LoD of 68.8 aM in CSF samples (plasma and serum samples were not tested). Overall, this innovative plastic antibody using molecular imprinting technology is specifically designed to detect aSyn monomers, offering the potential for early detection of PD by identifying the protein before the formation of aggregates. This study presents a new analytical tool that could be utilized for early and cost-effective PD diagnosis in future clinical applications.

CRediT authorship contribution statement

Inês S. da Silva: Writing – original draft, Methodology, Investigation, Formal analysis, Data curation. **Ana R. Cardoso:** Writing – review & editing, Writing – original draft, Visualization, Validation, Supervision, Investigation, Formal analysis, Data curation. **Lasse Reimer:** Writing – review & editing, Visualization, Methodology. **Annekatrin König:** Writing – review & editing, Visualization, Methodology. **Christoph van Riesen:** Writing – review & editing, Visualization, Methodology. **Tiago Fleming Outeiro:** Writing – review & editing, Visualization, Resources, Project administration, Methodology, Funding acquisition. **Poul Henning Jensen:** Writing – review & editing, Visualization, Resources, Project administration, Methodology, Funding acquisition, Formal analysis. **M. Goreti F. Sales:** Writing – review & editing, Visualization, Validation, Supervision, Resources, Project administration, Methodology, Funding acquisition, Conceptualization.

Declaration of competing interest

The authors declare that they have no known competing financial interests or personal relationships that could have appeared to influence the work reported in this paper.

Acknowledgements

The authors acknowledge funding received from the ERA-Net and the National Foundation for Science and Technology (FCT, JPCO-FUND2/0001/2019), as well as the EU Joint Programme – Neurodegenerative Disease Research (JPND) co-fund project, JPCOFUND2, under grant agreement no. 825664. ARC acknowledges funding FCT, through the PhD Grant SFRH/BD/130107/2017. TFO acknowledges funding to Deutsche Forschungsgemeinschaft (DFG, German Research Foundation) under Germany's Excellence Strategy - EXC 2067/1–390729940, by SFB1286 (B8) and by the BMBF through the EU Joint Programme on Neurodegenerative Disease Research (JPND, www.jpnd.edu) project (OligoFit).

Appendix ASupplementary data

Supplementary data to this article can be found online at https://doi.org/10.1016/j.bios.2024.116880.

Data availability

No data was used for the research described in the article.

References

An, Y., Tang, L., Jiang, X., Chen, H., Yang, M., Jin, L., Zhang, S., Wang, C., Zhang, W., 2010. Chem. Eur J. 16, 14439–14446. https://doi.org/10.1002/chem.201001654.

Anderson, J.P., Walker, D.E., Goldstein, J.M., De Laat, R., Banducci, K., Caccavello, R.J., Barbour, R., Huang, J., Kling, K., Lee, M., Diep, L., Keim, P.S., Shen, X., Chataway, T., Schlossmacher, M.G., Seubert, P., Schenk, D., Sinha, S., Gai, W.P., Chilcote, T.J., 2006. J. Biol. Chem. 281, 29739–29752. https://doi.org/10.1074/jbc.M600933200.

Brett, C.M.A., Èrgy Inzelt, G., Kertesz, V., 1999. Anal. Chim. Acta 385, 119–123. https://doi.org/10.1016/S0003-2670(98)00808-3.

Cardoso, A.R., de Sá, M.H., Sales, M.G.F., 2019a. Bioelectrochemistry 130, 107287. https://doi.org/10.1016/j.bioelechem.2019.04.017.

Cardoso, A.R., Marques, A.C., Santos, L., Carvalho, A.F., Costa, F.M., Martins, R., Sales, M.G.F., Fortunato, E., 2019b. Biosens. Bioelectron. 124–125, 167–175. https://doi.org/10.1016/j.bios.2018.10.015.

ChuangYe Ge, Md, Rahman, Mahbubur, Zhang, Wei, Nasrin Siraj Lopa, L.J., Sujin, Yoon, Jang, Hohyoun, Xu Guang-Ri, W.K., 2020. Sensors 20, 617. https://doi.org/10.3390/s20030617.

Donadio, V., Incensi, A., Leta, V., Giannoccaro, M.P., Scaglione, C., Martinelli, P., Capellari, S., Avoni, P., Baruzzi, A., Liguori, R., 2014. Neurology 82, 1362–1369. https://doi.org/10.1212/WNL.0000000000000316.

El-agnaf, O.M.A., Salem, S.A., Paleologou, K.E., Curran, M.D., Gibson, M.J., Court, J.A., Schlossmacher, M.G., Allsop, D., 2006. Faseb. J. 20 (3), 419–425. https://doi.org/10.1096/fj.03-1449com.

Eliezer, D., Kutluay, E., Bussell, R., Browne, G., 2001. J. Mol. Biol. 307, 1061–1073. https://doi.org/10.1006/jmbi.2001.4538.

Eusebi, P., Giannandrea, D., Biscetti, L., Abraha, I., Chiasserini, D., Orso, M., Calabresi, P., Parnetti, L., 2017. Movement Disorders 32, 1389–1400. https://doi.org/10.1002/mds.27110.

Fearnley, J.M., Lees, A.J., 1991. Brain 114, 2283–2301. https://doi.org/10.1093/brain/114.5.2283.

Harvey, D., 2000. Modern Analytical Chemistry. McGraw-Hill, Massachusetts, p. 816.

Hassan, Q., Li, S.P., Ferrag, C., Kerman, K., 2019. Anal. Chim. Acta 1089, 32–39. https://doi.org/10.1016/j.aca.2019.09.013.

Hughes, A.J., Daniel, S.E., Kilford, L., Lees, A.J., 1992. J. Neurol. Neurosurg. Psychiatry 55, 181–184. https://doi.org/10.1136/jnnp.55.3.181.

Kapaki, E., Paraskevas, G.P., Emmanouilidou, E., Vekrellis, K., 2013. PLoS One 8, 1–9. https://doi.org/10.1371/journal.pone.0081654.

Karyakin, A.A., Strakhova, A.K., Karyakina, E.E., Varfolomeyev, S.D., Yatsimirsky, A.K., 1993. Bioelectrochem. Bioenerg. 32, 35–43. https://doi.org/10.1016/0302459893800018P.

Koukouraki, P., Doxakis, E., 2016. Open Biol 6, 160022. https://doi.org/10.1098/rsob.160022.

Kumar, S.T., Jagannath, S., Francois, C., Vanderstichele, H., Stoops, E., Lashuel, H.A., 2020. Neurobiol. Dis. 146, 105086. https://doi.org/10.1016/j.nbd.2020.105086.
Kumari, P., Ghosh, D., Vanas, A., Fleischmann, Y., Wiegand, T., 2021. Proc. Natl. Acad. Sci. USA 118, 2–9. https://doi.org/10.1073/pnas.2012171118/-/DCSupplemental. Published.
Lee, M.H., Liu, K.T., Thomas, J.L., Su, Z.L., O'Hare, D., Van Wuellen, T., Chamarro, J.M., Bolognin, S., Luo, S.C., Schwamborn, J.C., Lin, H.Y., 2020. ACS Appl. Nano Mater. 3, 8027–8036. https://doi.org/10.1021/acsanm.0c01476.
Lee, M., Thomas, J.L., Su, Z., Yeh, W., Monzel, A.S., Bolognin, S., Schwamborn, J.C., Yang, C., Lin, H., 2021a. Biosens. Bioelectron. 175, 112852. https://doi.org/10.1016/j.bios.2020.112852.
Lee, M.H., Thomas, J.L., Su, Z.L., Yeh, W.K., Monzel, A.S., Bolognin, S., Schwamborn, J. C., Yang, C.H., Lin, H.Y., 2021b. Microchim. Acta 188, 203. https://doi.org/10.1007/s00604-021-04850-w.
Li, X., Dong, C., Hoffmann, M., Garen, C.R., Cortez, L.M., Petersen, N.O., Woodside, M.T., 2019. Sci. Rep. 9, 1734. https://doi.org/10.1038/s41598-018-37584-6.
Lindersson, E., Beedholm, R., Højrup, P., Moos, T., Gai, W.P., Hendil, K.B., Jensen, P.H., 2004. J. Biol. Chem. 279, 12924–12934. https://doi.org/10.1074/jbc.M306390200.
Liu, J., Mu, S., 1999. Synth. Met. 107, 159–165. https://doi.org/10.1016/S0379-6779(99)00146-0.
Liu, W.W., Zhu, Y., Fang, Q., 2017. Anal. Chem. 89, 6678–6685. https://doi.org/10.1021/acs.analchem.7b00899.
Liu, Y., Hu, X., Xia, Y., Zhao, F., Zeng, B., 2022. Anal. Chim. Acta 1190, 336245. https://doi.org/10.1016/j.aca.2021.339245.
Ma, Y., Hu, Q., Liu, C., Wang, L., 2020. J. Electroanal. Chem. 862, 113994. https://doi.org/10.1016/j.jelechem.2020.113994.
Maass, F., Rikker, S., Dambeck, V., Warth, C., Tatenhorst, L., Csoti, I., Schmitz, M., Zerr, I., Leha, A., Bähr, M., Lingor, P., 2020. Sci. Rep. 10, 8507. https://doi.org/10.1038/s41598-020-65503-1.
Maroteaux, L., Campanelli, J.T., Scheller, R.H., 1988. J. Neurosci. 8, 2804–2815. https://doi.org/10.1523/jneurosci.08-08-02804.1988.
Pilvenyte, G., Ratautaite, V., Boguzaite, R., Samukaite-Bubniene, U., Plausinaitis, D., Ramanaviciene, A., Bechelany, M., Ramanavicius, A., 2023. J. Pharm. Biomed. Anal. 228, 115343. https://doi.org/10.1016/j.jpba.2023.115343.
Polymeropoulos, M.H., Lavedan, C., Leroy, E., Ide, S.E., Dehejia, A., Dutra, A., Pike, B., Root, H., Rubenstein, J., Boyer, R., Stenroos, E.S., Chandrasekharappa, S., Athanassiadou, A., Papapetropoulos, T., Johnson, W.G., Lazzarini, A.M., Duvoisin, R. C., Di Iorio, G., Golbe, L.I., Nussbaum, R.L., 1997. Science 276, 2045–2047. https://doi.org/10.1126/science.276.5321.2045.
Postuma, R.B., Berg, D., 2017. Chapter 4 - the new diagnostic criteria for Parkinson's disease. Int. Rev. Neurobiol. 132, 55–78. https://doi.org/10.1016/bs.irn.2017.01.008.
Proceedings of Synuclein Meeting 2022. In: Resumos em Livros de Atas / Abstracts in Proceedings, of the Synuclein Meeting, Leuven/Belgium, 2022. CEB. https://repositorium.sdum.uminho.pt/handle/1822/77520.
Rebelo, T.S.C.R., Pereira, C.M., Sales, M.G.F., Noronha, J.P., Silva, F., 2016a. Electrochim. Acta 190, 887–893. https://doi.org/10.1016/j.electacta.2015.12.214.
Rebelo, T.S.C.R., Pereira, C.M., Sales, M.G.F., Noronha, J.P., Silva, F., 2016b. Sens actuat. Biol. Chem. 223, 846–852. https://doi.org/10.1016/j.snb.2015.09.133.
Reimer, L., Haikal, C., Gram, H., Theologidis, V., Kovacs, G., Ruesink, H., Baun, A., Nielsen, J., Otzen, D.E., Li, J.Y., Jensen, P.H., 2022. Sci. Rep. 12, 3737. https://doi.org/10.1038/s41598-022-07706-2.
Ruesink, H., Reimer, L., Gregersen, E., Moeller, A., Betzer, C., Jensen, P.H., 2019. PLoS One 14, e0216764. https://doi.org/10.1371/journal.pone.0216764.
Serrano, V.M., Silva, I.S.P., Cardoso, A.R., Sales, M.G.F., 2022. Chemosensors 10, 189. https://doi.org/10.3390/chemosensors10050189.
Shalash, A., Salama, M., Makar, M., Roushdy, T., Elrassas, H.H., Mohamed, W., El-Balkimy, M., Donia, M.A., 2017. Front. Neurol. 8, 720. https://doi.org/10.3389/fneur.2017.00720.
Siderowf, A., Concha-Marambio, L., Lafontant, D.E., Farris, C.M., Ma, Y., Urenia, P.A., Nguyen, H., Alcalay, R.N., Chahine, L.M., Foroud, T., Galasko, D., Kieburtz, K., Merchant, K., Mollenhauer, B., Poston, K.L., Seibyl, J., Simuni, T., Tanner, C.M., Weintraub, D., Videnovic, A., Choi, S.H., Kurth, R., Caspell-Garcia, C., Coffey, C.S., Frasier, M., Oliveira, L.M.A., Hutten, S.J., Sherer, T., Marek, K., Soto, C., 2023. Lancet Neurol. 22, 407–417. https://doi.org/10.1016/S1474-4422(23)00109-6.
Silva, I., Cardoso, A.R., Sales, M.G., 2024. Electrochemical biosensor-based detection assays for early diagnosis of neurodegenerative disorders. In: Parihar, A., Khan, R., Srivastava, A.K. (Eds.), Chapter 7 in Smart Diagnostics for Neurodegenerative Disorders, s. Elsevier. https://doi.org/10.1016/B978-0-323-95539-3.00010-7.
Spillantini, M.G., Schmidt, M.L., Lee, V.M., Trojanowski, J.Q., M, J.R., G, 1997. Nature 388, 839–840. https://doi.org/10.1038/42166.
Stephens, A.D., Zacharopoulou, M., Moons, R., Fusco, G., Seetaloo, N., Chiki, A., Woodhams, P.J., Mela, I., Lashuel, H.A., Phillips, J.J., De Simone, A., Sobott, F., Schierle, G.S.K., 2020. Nat. Commun. 11, 2820. https://doi.org/10.1038/s41467-020-16564-3.
Sunon, P., Ngamchuea, K., 2023. Microchim. Acta 190, 348. https://doi.org/10.1007/s00604-023-05930-9.
Teunissen, C.E., Petzold, A., Bennett, J.L., Berven, F.S., Brundin, L., Comabella, M., Franciotta, D., Frederiksen, J.L., Fleming, J.O., Furlan, R., Hintzen, R.Q., Hughes, S. G., Johnson, M.H., Krasulova, D.E., Kuhle, J., Magnone, M.C., Rajda, C., Rejdak, K., Schmidt, H.K., Van Pesch, V., Waubant, E., Wolf, C., Giovannoni, G., Hemmer, B., Tumani, H., Deisenhammer, F., 2009. Neurol. J. 73, 1914–1922. https://doi.org/10.1212/WNL.0b013e3181c47cc2.
Van Den Eeden, S.K., Tanner, C.M., Bernstein, A.L., Fross, R.D., Leimpeter, A., Bloch, D. A., Nelson, L.M., 2003. Am. J. Epidemiol. 157, 1015–1022. https://doi.org/10.1093/aje/kwg068.
Xia, Y., De Rohan Suva, H.A., Rosi, B.L., Yamaoka, L.H., Rimmler, J.B., Pericak-Vance, M. A., Roses, A.D., Chen, X., Masliah, E., Deteresa, R., Iwai, A., Sundsmo, M., Thomas, R.G., Richard Hofstetter, C., Gregory, E., Hansen, L.A., Katzman, R., Thai, L. J., Saitoh, T., 1996. Ann. Neurol. 40, 207–215. https://doi.org/10.1002/ana.410400212.
Xu, Q., Cheng, H., Lehr, J., Patil, A.V., Davis, J.J., 2015. Anal. Chem. 87, 346–350. https://doi.org/10.1021/ac503890e.
Yan, S., Jiang, C., Janzen, A., Barber, T.R., Seger, A., Sommerauer, M., Davis, J.J., Marek, K., Hu, M.T., Oertel, W.H., Tofaris, G.K., 2024. JAMA Neurol. 81, 59–68. https://doi.org/10.1001/jamaneurol.2023.4398.
Zhu, J., Cui, Y., Zhang, J., Yan, R., Su, D., Zhao, D., Wang, A., Feng, T., 2024. Lancet Healthy Longev 5, e464–e479. https://doi.org/10.1016/S2666-7568(24)00094-1.